MECP2 expression coincides with age-dependent tactile sensory deficits in a female mouse model for Rett syndrome

Michael Mykins[1*], Dana Layo-Carris[1*], Logan Dunn[1*], Sarah Perez, Alexandra Mcbryar, Billy You Bun Lau[1], Keerthi Krishnan[1]

[1] Department of Biochemistry & Cellular and Molecular Biology, University of Tennessee Knoxville,

* Co-First Authors

Corresponding author: Dr. Keerthi Krishnan, krishnan@utk.edu

ORCiD #:
KK: 0000-0002-0858-4624
BYBL: 0000-0002-2380-5341
MM: 0000-0003-3467-5308
DLC: 0000-0001-7009-0652
LD: 0000-0002-2147-5502

Contributions:

KK and DLC designed the study. DLC performed tactile behavior. LD, MM, and BYBL performed 6-week-old consecutive maternal behavior. BYBL scored maternal behavior. LD performed confocal imaging and MECP2 analysis. DLC, AM and SP performed data quantification in Datavyu. MM designed the R studio codes for analysis and data visualization of tactile behavioral data. DLC performed immunohistochemistry and epifluorescent PNN imaging for 6wk naïve animals. DLC, AM and SP performed mapping and PNN high intensity count analysis for 6wk naïve animals. MM and LD performed statistical analysis, and generated data visualizations in R studio and GraphPad, respectively. MM, LD, DLC, BYBL and KK contributed to in-depth discussions, and wrote the paper.

Abstract:

Rett syndrome is characterized by an early period of typical development and then, regression of learned motor and speech skills in girls. The underlying mechanisms from normalcy to regression are unclear. Due to random X-chromosome inactivation, female patients of Rett syndrome, and female mouse models of Rett syndrome (*Mecp2*^{Heterozygous}, Het) express a functional copy of wild-type MECP2 protein in half of all mature cells in brain and body. By analyzing wild-type MECP2 expression in the context of whisker tactile sensory perception, here we report compensatory increase in MECP2 protein expression in 6-week-old adolescent Het mice, which display normal levels of perineuronal net expression, mild tactile sensory perception deficit and efficient pup retrieval behavior. Comparatively, 12-week-old adult Het mice display decreased MECP2 expression and significant tactile sensory perception deficits. Thus, we have identified a period of normalcy and regression in this female mouse model, which coincide with variable wild-type expression of MECP2. We speculate that compensatory increases in MECP2 expression in Het brains allows for normal functioning, while the inability to maintain these expression level changes leads to behavioral deficits.

Introduction:

Disruption of primary sensory processing is evident in X-linked neurodevelopmental disorders such as Autism Spectrum Disorder and Rett syndrome (Buchanan et al., 2019; Djukic et al., 2012; Djukic & Valicenti McDermott, 2012; Key et al., 2019; LeBlanc et al., 2015; Merbler et al., 2020; Nomura, 2005; Peters et al., 2015; Symons et al., 2019). Such disruptions during development and adulthood likely contributes to motor dysfunction and social communication deficits in girls and women with Rett syndrome. Stereotypic features of Rett syndrome include typical infancy, regression with sensory, motor, speech and cognitive issues (Bebbington et al., 2008; Buchanan et al., 2019; Djukic et al., 2012; Djukic & Valicenti McDermott, 2012; Nomura, 2005). Mutations in the X-linked gene, methyl-CPG-binding protein 2 (MECP2) are associated with Rett syndrome (Amir et al., 1999). Atypical sensory processing phenotypes have been reported predominantly in developing male *Mecp2*-null rodent models for Rett syndrome (Durand et al., 2012; Ito-Ishida et al., 2015, p.; Krishnan et al., 2015; Lee et al., 2017; Lo et al., 2016; Orefice et al., 2016). However, the impact of this early developmental deficiency on adolescent and adult brain and body function is unclear, due to the overall poor health and early lethality of the null male mice. The extent of tactile sensory processing phenotypes in female heterozygous mouse models, the appropriate genotype to model Rett syndrome, is unclear. This is a particularly important consideration as MECP2, is located on the X-chromosome and is subject to random X–chromosome inactivation. As a result, MECP2 protein is expressed in a mosaic pattern, where individual cells express either the wild-type protein or no/deficient protein across the brain and body. Due to this inherent mosaicism, girls/women with Rett syndrome and individual female heterozygous mice (*Mecp2* ^{heterozygous}, Het) are highly variable. Thus, the impact of mosaic MECP2 expression in Het is fundamentally different than in male *Mecp2*-null mice, due to likely compensation and adaptations in the neural circuitry from early development to adulthood.

In wild-type primary sensory cortices, MECP2 expression increases postnatally, concomitant with the emergence of appropriate critical periods, and is thought to be stable in adolescence and adulthood (Braunschweig, 2004; Skene et al., 2010; Yagasaki et al., 2018). At the cellular level, MECP2 is highly expressed in GABAergic interneurons over pyramidal neurons of the same region (Ito-Ishida et al., 2015; Takei et al., 2021) . Surprisingly, MECP2 expression in Het sensory cortices, with cell type resolution, is unknown. Due to its significant roles in gene regulation (Chahrour et al., 2008; Chen et al., 2015; Fuks et al., 2003; Gabel et al., 2015; Jones et al., 1998; Klose et al., 2005; Lyst & Bird, 2015; Tao et al., 2009; Zhou et al., 2006) and the timing of experience-dependent plasticity (Krishnan et al., 2015, 2017; Lau, Krishnan, et al., 2020; Morello et al., 2018; Noutel et al., 2011; Patrizi et al., 2020; Picard & Fagiolini, 2019), investigation of MECP2 expression in female heterozygous mice across ages is essential to unravel the mechanisms connecting genotype to phenotype.

Previously, we have established an ethologically relevant maternal behavior paradigm to characterize auditory processing, tactile sensory processing, motor and social communication phenotypes in Het (Krishnan et al., 2017; Lau, et al., 2020; Stevenson et al., 2021). Adult Het are inefficient at pup retrieval task conducted over three or six days (Krishnan et al., 2017; Stevenson et al., 2021). We identified dysregulation of the parvalbumin+ GABAergic neurons (PV) in auditory and primary somatosensory cortices as a key cellular substrate for this inefficient pup retrieval (Krishnan et al., 2017; Lau et al., 2020a). Of particular interest is the barrel field of the primary somatosensory cortex (S1BF), which receives peripheral whisker stimulation input and is important for tactile sensory perception. We found an atypical

increased expression of specialized extracellular matrix structures called perineuronal nets (PNNs) in adult Het S1BF (Lau et al., 2020). PNNs ensheath PV neuron soma and proximal dendrites and regulate their synaptic plasticity (de Vivo et al., 2013; Hartig et al., 1992; Pizzorusso et al., 2002; Ueno et al., 2018), suggesting that increased PNN expression could hinder the processing of whisker sensation. Furthermore, systematic analysis of goal-related movements during pup retrieval showed adult Het approached the pups more and interacted more than adult littermate wild-type controls (WT), suggesting possible tactile hyposensitivity in adult Het (Krishnan et al., 2017; Stevenson et al., 2021).

Here, we test the tactile hyposensitivity phenotype in adolescent and adult Het by using systematic frame-by-frame analysis of texture investigation and object investigation tasks. Adult Het interacted with textures, but not objects, more and for longer times than WT. Surprisingly, adolescent Het behaved similarly to adolescent WT, in both pup retrieval and tactile assays, suggesting that tactile hyposensitivity in Het are age-related. Furthermore, PNN expression in S1BF correlated with the tactile phenotypes in an age-appropriate manner. Surprisingly, in non-PV cells, we found an atypical increase in MECP2 expression in adolescent Het S1BF and a decrease in adult S1BF, suggesting that cells expressing MECP2 in Het engage in age-specific compensatory mechanisms, which coincides with behavioral phenotype. MECP2 expression in Het PV neurons are unchanged with age. Together, these are novel results, which open up new directions of exploration on the role of cell type-specific MECP2 expression, regulation and function in Het over time.

Materials and Methods:

Animals

We used the following mouse strains: CBA/CaJ (JAX:000654), *Mecp2*^{Het} (C57BL6/J, B6.129P2(C)-*Mecp2*$^{tm1.1Bird}$/J, JAX:003890) (Guy et al., 2001)and *Mecp2*^{WT} siblings. All animals were same-sex group-housed after weaning, raised on a 12/12-hour light/dark cycle (lights on at 7 am) and received food ad libitum. Behavioral experiments were performed using female *Mecp2*^{WT} (WT) and *Mecp2*^{Het} (Het) at either 6 or 10-12(collectively called 12) weeks of age between the hours of 9 am and 6 pm (during light cycle). 10-12 week-old CBA mothers were used for pup retrieval task. All procedures were conducted in accordance with the National Institutes of Health's Guide for the Care and Use of Laboratory Animals and approved by the University of Tennessee-Knoxville Institutional Animal Care and Use Committee.

Pup retrieval task:

Behavioral Setup:

The pup retrieval task was performed as previously described (Krishnan et al., 2017; Lau, et al., 2020a; Lau et al., 2020b; Stevenson et al., 2021). Two 5-week-old naïve females, WT and Het, were co-housed with a pregnant CBA/CaJ female 3-5 days before birth; these naive females were then termed 'surrogate'. Once the pups were born (postnatal day 0; P0), we performed the pup retrieval task with these 6-week old surrogates. The behavior was performed in the home cage, which was placed inside a sound- and light-proof box as follows: one surrogate was placed in the home cage with 3-5 pups (*habituation*; 5 minutes), the pups were removed from the nest (*isolation*; 2 minutes), and the pups were scattered throughout the home cage by placing them in the corners and center, allowing the surrogate to retrieve pups back to the nest (*retrieval*; 5 minutes). The nest was left empty, if there were fewer than five pups. The assay was performed in the dark and recorded using infrared cameras during all phases of each trial. This behavior was tested for six consecutive days. If not all pups were retrieved to the nest by the 5-minute mark, we placed pups back in the nest in preparation for the next surrogate. After the behavior was completed, all mice were returned to the home cage.

Pup retrieval task Analysis:

All videos were coded so the analyzers were blind to the identity of the mice. Each video was manually scored for latency (the amount of time required to retrieve all pups back to the nest out of 5 minutes) and the number of errors (surrogate-pup interactions not resulting in successful retrieval). Latency was calculated as:

$$\textit{Latency index} = [(t_1 - t_0) + (t_2 - t_0) + \ldots + (t_n - t_0)] / (n \times L)$$

Where n = number of pups outside the nest, t_0 = start of trial (s), t_n = time of the nth pup's successful retrieval to the nest (s), L = trial length (300 s). Statistical analyses and figures were generated using GraphPad Prism.

Tactile Perception Tasks:

Behavioral Setup:

WT and Het underwent a five-day battery of behavioral tests to assay tactile processing through the whiskers (Figure 2). The behavior chamber used for tactile assays was a 40 x 40 x 40 cm plexiglass box with two sets of holes in the center of the plexiglass floor for the texture/object inserts. Holes were drilled to be equidistant from the center, with a 4.0 cm spacing between hole sets. Texture discrimination plexiglass inserts were 0.5 cm (thickness) x 4.0 cm (width) x 15.0 cm (height). Rodents use their whiskers to both detect and discriminate between textures and objects (Rodgers et al., 2021). We chose to test the ability of experimental mice to discriminate between textures using both large and small textural differences. Sandpaper textures were designed to slide on and off the inserts to be cleaned between animals. The textures were made of 3M sandpaper of varying grit: a course 60-grit, a medium 120-grit, and a fine 220-grit. Inserts used for novel object recognition were plexiglass spheres (4.0 cm diameter) and plexiglass cubes (4.0 cm^3) (Orefice et al., 2016; Wu et al., 2013). The chamber and inserts were cleaned with MB-10 and allowed to dry completely before the start of each behavior, and an additional 5-minute period was allotted between tests to eliminate scent biases. All behaviors were performed in the dark and recorded with an infrared camera.

Behavioral Paradigm (Figure 2):

Habituation: On days 1 and 2 of behavior, a mouse was placed into the behavior chamber for 10 minutes to familiarize with the new environment. One 10-minute trial was performed on each day. Tape was placed over the drilled holes in the chamber floor to prevent potential injuries from occurring.

Texture Discrimination: On days 3 and 4, texture discrimination began with a familiarization trial. Experimental mice were placed one-at-a-time into the chamber with two identical texture inserts and allowed to investigate. After the first 10-minute trial, the mouse was returned to the home cage for a 5-minute period. During this time, textures and inserts for familiarization were replaced with new sets of inserts and textures for use in the testing trial. After 5 minutes, the mouse was returned to the behavior chamber for a second trial and filmed for a total of 10 minutes (testing phase). Familiarization phases of each behavior were performed using two course texture inserts (60-grit). During testing phase on days 3 and 4, we replaced one insert with a medium (120-grit) and fine (220-grit) texture insert, respectively.

Novel Object Recognition: On day 5, a novel object recognition assay was performed following a paradigm, similar to the texture discrimination assay with minor changes. The familiarization trial was performed using a set of two 4.0 cm^3 plexiglass cubes. For the testing trial, the set of familiarization cubes were replaced by a plexiglass object set consisting of one cube and one sphere.

Tactile Behavior Analysis: Behaviors for both texture and object investigation were manually scored using Datavyu software (2014), all analyzers were blinded to the age and genotype of the mice. The videos were scored for the time intervals in which the mouse interacted with the novel and familiar textures / objects throughout the 10-minute

Whisker	- Within 3 cm of the object and actively exploring around texture/object - Clear whisker contact with texture/object
Whole-body climbing	- All four paws are off the ground and animal is climbing the texture/object
Forepaw	- Touching the object/texture with forepaws while the hind limbs are contacting the ground

Table 1. *Definitions of parameters used to score behaviors.*

testing trial. We classified interactions into three categories, as shown in Table 1, based on pilot observations and previous studies (Orefice et al., 2016; Pacchiarini et al., 2017; Wu et al., 2013). We excluded mice from analysis if the investigation time of textures / objects during a given trial did not exceed 2 seconds (Orefice et al., 2016; Patrick Wu & Dyck, 2018). After manual scoring, interaction sequences for each animal were extracted from Datavyu for quantitative analyses. Number of animals included in the analysis for each behavioral day and number of animals excluded for those days are described in Table 2.

We separated contacts, investigation time and duration per interactions with textures/objects into whisker, forepaw and whole-body climbing for each animal. Duration per interaction was calculated by taking the time difference between the end and start of an interaction. Our results are reported as raw number of contacts, raw investigation times, and raw duration per interaction split by interaction type, age and genotype. We conducted unpaired Mann Whitney-U tests to determine statistical significance between genotypes and across ages within the same genotype. Statistical analysis and data visualization were performed in R studio.

		Included in analysis		**Excluded In analysis**	
		WT	Het	WT	Het
12 wk	Texture Discrimination Day 1	8	7	1	1
	Texture Discrimination Day 2	8	8	1	0
	Novel Object Recognition	9	8	0	0
	Adhesive Test	9	8	0	0
6 wk	Texture Discrimination Day 1	8	8	1	2
	Texture Discrimination Day 2	9	10	1	0
	Novel Object Recognition	9	10	0	0
	Adhesive Test	9	10	0	0

Table 2. *Number of animals included in and* ***excluded*** *from analysis. Animals were excluded from analysis due to technical difficulties with video lagging/skipping or no interactions with textures.*

Immunohistochemistry

All animals were perfused with a 4% paraformaldehyde/PBS solution after behavior. Extracted brains were stored in 4% paraformaldehyde/PBS solution overnight at 4°C and furthered processed in cohorts (one WT and one Het) as previously described (Lau et al., 2020). Briefly, coronal brain sections (100 µm thickness) encompassing the entire primary somatosensory cortex were collected using a freezing microtome. We denoted the left hemisphere by poking a small hole in the ventral part of the brain. Free-floating

sections were blocked with 10% normal goat serum, 0.5% Triton X-100 solution, followed by incubation with biotin-conjugated WFA lectin (1:500; Sigma-Aldrich) and rabbit MECP2 primary antibody (1:1,000; Cell Signaling), then with secondary antibodies conjugated with AlexaFluor-488 and Texas-Red (1:1,000; Invitrogen) to label PNNs and MECP2, respectively, and counterstained with DAPI before mounting section onto slides.

Microscopy and Image Analysis

Image Acquisition

PNN: Each hemisphere of the brain section was single-plane imaged at 10x using Keyence epifluorescence microscope (Keyence BZ-X710; Keyence Corp.) and stitched using BZ-X Analyzer (Keyence). We determined imaging settings for each cohort based on Het PNN intensity. To reduce overexposure, we set the exposure time to the point when the first saturated pixel appeared in the sample, then reduced the exposure time by one unit (based on the software). This procedure was performed in both hemispheres for all Het sections, and the lowest exposure time occurring most frequently was used to image all sections within that cohort.

MECP2 and DAPI: Image acquisition of MECP2 expression and DAPI was performed using a VT-Hawk 2D-array scanning confocal microscope (Visitech intl.) mounted to an IX-83 inverted optical microscope (Olympus). Z-series images with a step interval of 0.5 µm were collected using a 60X/numerical aperture 1.40 Plan APO VC objective lens (Nikon) in MetaMorph (Molecular Devices). Settings for each laser channel were determined in a similar manner as previously described for PNNs while utilizing the histogram function in MetaMorph. Settings were determined using the top 25.0 µm of tissue. All confocal images were collected with a standardized set of channel settings in the 16-bit range. Images were collected from the Layer IV barrel field subregion in both hemispheres of two sections.

Image Processing & Analysis

PNN: The density of high-intensity PNNs were quantified as previously described (Lau et al., 2020b) using ImageJ (Schneider et al., 2012). Briefly, each stitched image (output from Keyence software as an RGB image) was overlaid with the corresponding coronal map template from mouse atlas (Paxinos & Franklin, 2013) and the total SS1 and its sub regions were outlined. High-intensity PNNs were quantified by maximizing the contrast of each image and manually marking the signals that were 80% or more of the original PNN. We divided the number of high-intensity PNNs by the area of the sub-region to calculate high-intensity PNN density. Statistical analyses and figures were generated using GraphPad Prism.

MECP2 and DAPI: Nuclear expression of MECP2 was quantified using ImageJ (Schneider et al., 2012). For background subtraction, a duplicate of the original image was created and processed by applying a median filter with a 32-pixel radius. The filtered image was then subtracted from the original image using the Image Calculator tool to produce 16-bit images for quantification. MECP2 expression was quantified within individual nuclei by creating 3.0-5.0 maximum intensity projections (16-bit greyscale) within the top 25.0 µm of each tissue. Projections were created for both the DAPI and MECP2 channels for ROI creation using the Polygon drawing tool and for quantification, respectively. DAPI, PNN+/- cells and MECP2-expressing cells were identified using merged tricolor images. Statistical analyses and figures were generated using GraphPad Prism.

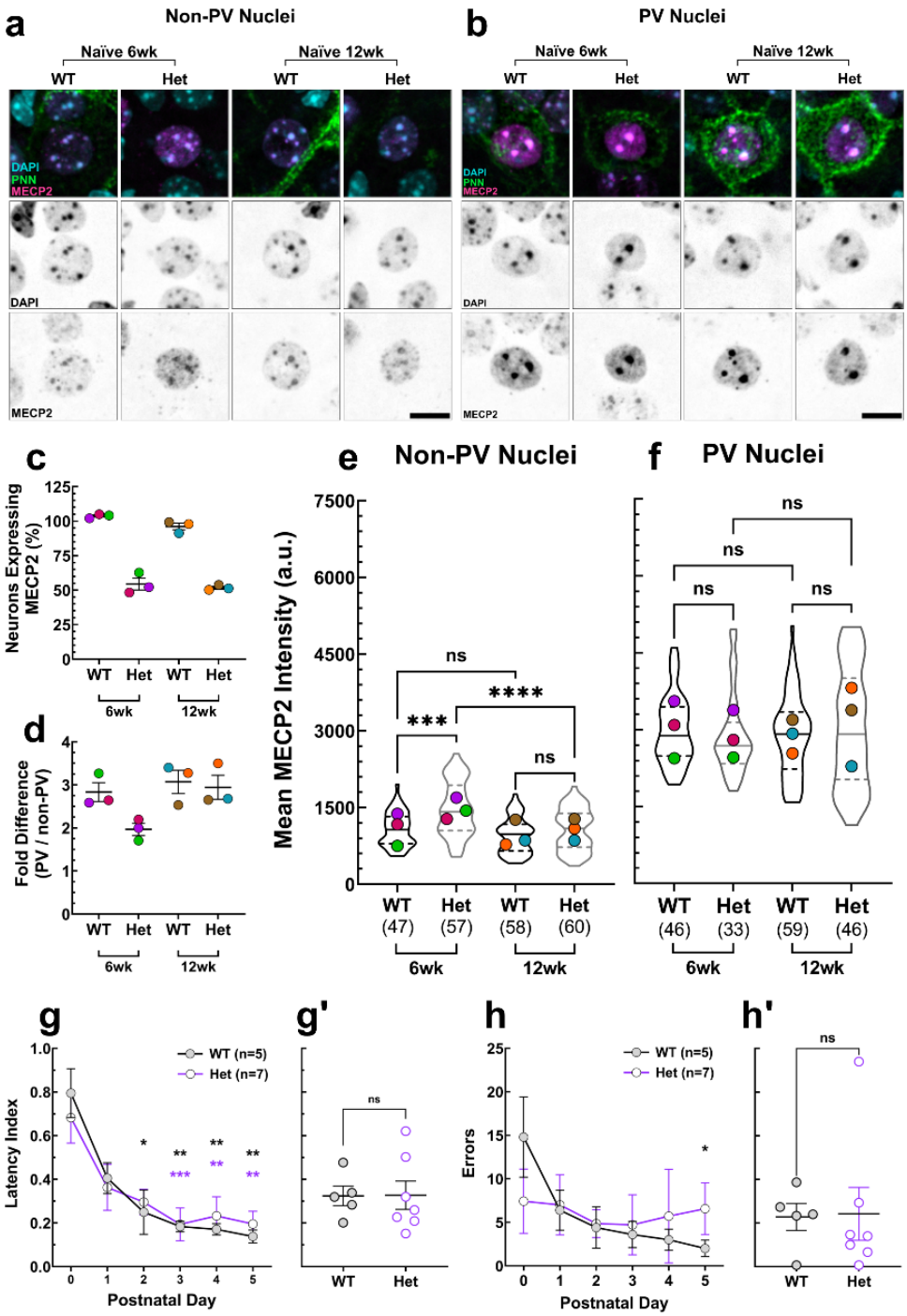

Results:

MECP2 expression is dynamically regulated in Het over time and cell types:

MECP2 protein expression varies in different cortical cell types (Ito-Ishida et al., 2015; Takei et al., 2021). It is currently unknown if cell type-specific MECP2 expression is stable over age, and if wild-type MECP2 expression in Het is similar to the age-matched controls (WT). Braunschweig et al, previously showed that wild-type MECP2 expression is decreased in Het; however, the brain region and age were not reported (Braunschweig, 2004). Thus, we performed

Figure 1. ***MECP2 is expressed differentially between cell types in S1BF of adolescent and adult WT and Het.*** Representative confocal images of nuclei stained with DAPI and MECP2 from **(a.)** non-PV (PNN-negative cells) putatively pyramidal neurons and **(b.)** PNN-positive parvalbumin (PV) interneurons. MECP2 intensity is higher within PV nuclei across ages; non-PV nuclei of adolescent (6wk) Het appear more intense compared to age-matched WT or adult (12wk) Het. Scale bars = 10um. **(c.)** Het express MECP2 in approximately 50% of neuronal nuclei, compared to WT across ages, as measured by percentage of MECP2-positive nuclei in adolescent and adult WT and Het (N = 4 images per brain, 3 brains per condition). **(d.)** Mean intensity of MECP2 protein from PV and non-PV nuclei is represented as a fold difference. **(e-f.)** Superplots representing the mean intensity of nuclear MECP2 of **(e)** non-PV and **(f)** PV interneurons within S1BF Layer IV of adolescent and adult WT and Het. In non-PV nuclei, 6-week-old Het show significant increase in MECP2 intensity, compared to age-matched WT, and a significant decrease with 12-week-old Het. PV nuclei did not show any significant differences in the higher MECP2 mean intensity across genotypes or age. Each colored circle represents an individual brain for each condition. Respective ages are indicated on the x-axis, and number of nuclei is shown in parentheses for each condition. *Kruskal-Wallis followed by Dunn's test: ns = not significant, ***p < 0.001, ****p < 0.0001.* **(g-g'.)** Mean latency index of pup retrieval behavior for each testing day (g) and averaged across all testing days (g') showed improved retrieval across testing days and no significant difference in average latency between genotypes. **(h-h'.)** Mean number of errors during pup retrieval for each testing day (h) and averaged across all testing days (h') showed no significant difference between genotypes. **(g-h.)** *Kruskal-Wallis followed by Dunn's test; *p < 0.05, **p < 0.01, ***p < 0.001, ****p < 0.0001.* Color * = within genotype, significance between P0 and P-day. **(g',h'.)** *Mann-Whitney test: ns = not significant.* Error bars represent ± SEM.

immunofluorescent staining and confocal microscopy to first characterize MECP2 expression in wild type and Het female mice during adolescence and adulthood within individual nuclei of the cortex. We chose to investigate expression in Layer IV of S1BF, the input layer from the whiskers, due to their importance in tactile sensory perception.

Consistent with previous observations, PNN-positive PV nuclei exhibited a roughly 3.0-fold higher level of MECP2 than non-PV nuclei in WT S1BF across adolescence and adulthood (6wk = 2.8±0.2; 12wk = 3.1±0.3) (Figure 1a-b, d-e). We did not detect significant changes in MECP2 expression between ages in either cell type of WT (Figure 1d-e). In Het, approximately 50% of cortical nuclei (identified by DAPI staining) within individual mice expressed wild-type MECP2 protein at both ages due to random X-chromosome inactivation (Figure 1c). Similar to WT, MECP2 expression in Het was higher in PV nuclei than non-PV nuclei in both ages (6wk = 2.0±0.1; 12wk = 2.9±0.3) (Figure 1a-b, d-e). Considering mean MECP2 intensity within non-PV nuclei, we found that adolescent Het expressed significantly higher MECP2 levels than age-matched WT (Figure 1d). Comparing Het female between ages, MECP2 levels of non-PV nuclei significantly decreased in 12-week-old adult Het (to levels consistent with age-matched WT females) from the originally higher levels observed in 6-week-old adolescent Het. MECP2 expression in PV nuclei did not change in adolescent or adult Het (Figure 1f), or across ages in WT in non-PV or PV nuclei (Figure 1e, f). Together, these results point to compensatory increase in MECP2 expression in non-PV nuclei expressing MECP2 in adolescent stage, and an inability to maintain the increased MECP2 expression in adult Het.

We hypothesized that the age-dependent decrease of MECP2 observed in adult Het contributed to the inefficient pup retrieval we had reported earlier (Krishnan et al., 2017; Stevenson et al., 2021). Thus, we performed the pup retrieval task on 6-week-old adolescent females. Adolescent Het and WT were comparably efficient at pup retrieval across six consecutive days of testing and on average, as measured by time to retrieve scattered pups to the nest (latency index; Figure 1f, f') and in pup interactions during retrieval (number of errors; Figure 1g, g'). Together, these results suggest that Het are capable of performing complex behavioral tasks over days, similar to WT, likely due to the compensatory increase in MECP2 expression in non-PV neurons of S1BF during adolescence.

Het display regression in whisker tactile sensory behavior from adolescent to adulthood:

Pup retrieval task involves multisensory integration of smell, hearing and tactile sensations, and motor coordination, which involves multiple brain regions and neural circuits. In order to focus specifically on

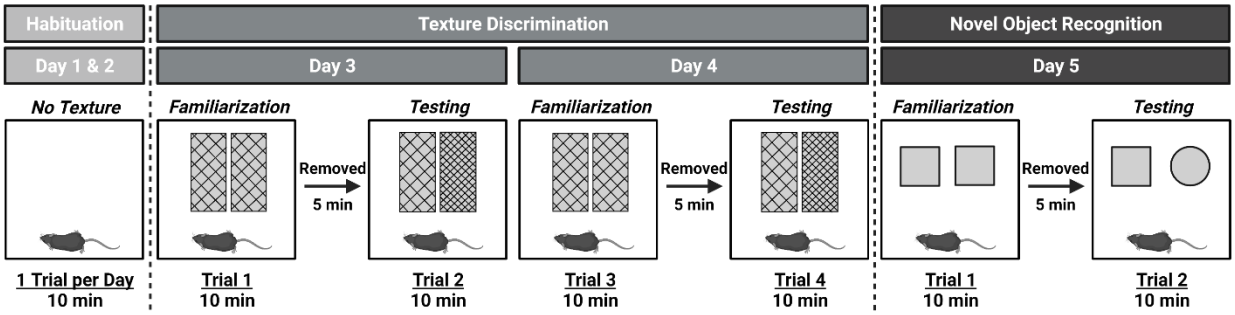

Figure 2. Tactile behavior schema. Behavior tests begin with two days to introduce the mice to the behavioral box set up. On each days of texture discrimination (days 3 and 4), individual mouse undergoes a 10-minute familiarization trial followed by a 10-minute testing trial, with varied sandpaper grits. On day 5, objects are used instead of textures for novel object recognition task. See Methods for detail.

whisker tactile perception and its connection to the S1BF, we performed standard texture discrimination and object recognition tasks on adolescent and adult WT and Het, and analyzed frame-by-frame with DataVyu software (Figure 2). We chose to perform a systematic analysis of all interactions, as mice interact with objects and textures with high speed, and rarely linger for the exploration (Figure 3a). At 6 weeks of age, WT and Het females predominantly investigate textures with multiple number of contacts with whiskers (Figure 3b). However, though the total time with textures did not differ significantly between WT and Het (Figure 3c); the duration per whisker interaction was significantly higher in adolescent Het (Figure 3d).

We performed similar analyses with novel object recognition to determine if adolescent Het are deficient in other forms of sensory dependent tasks. Adolescent WT and Het used their whiskers, forepaws, and whole-body climbing to investigate objects (Figure 4a). Interestingly, compared to adolescent WT, adolescent Het made less whisker contacts (Figure 4b) and spent the same total time investigating objects (Figure 4e). There was no significant difference in the number of contacts or time spent investigating objects using forepaws (Figure 4c, f) and whole-body climbing (Figure 4d, g). Similar to texture investigation, compared to adolescent WT, adolescent Het interacted significantly longer per interaction using whiskers (Figure 4h) but not forepaws or whole-body climbing (Figure 4i, j). Together, the increased duration of interactions when interacting with textures and objects suggest the beginnings of a mild whisker hyposensitivity in adolescent Het.

Percentage of time spent with different textures did not change in adolescents during texture investigation (WT: 50.14% +/- 4.344, n=9: Het: 55.60% +/- 4.116, n=10; one sample t-test with 50% chance)_or with objects during object investigation (WT: 47.74% +/- 4.263, n=9: Het: 50.33% +/- 3.572, n=10; one sample t-test with 50% chance). Percentage of time spent with textures did not change in adult WT or Het female mice (WT: 57.08% +/- 3.356, n=9: Het: 51.59% +/- 3.531, n=8; one sample t-test with 50% chance) and during object investigation (WT: 51.67% +/- 4.477, n=9: Het: 57.26% +/- 4.511, n=8; one sample t-test with 50% chance). Thus, we refrain from speculating about preferences of the female mice or their memory.

On the contrary, adult Het displayed significant whisker hyposensitivity, compared to adult WT (Figure 5). Examples of frame-by-frame sequence analysis show that non-whisker interactions are interspersed with whisker interactions in adult Het (Figure 5a). All the adult WT continue to use their whiskers to interact fleetingly with textures, while most of the adult Het used whiskers, forepaw and whole body climbing to interact with the textures. Compared to WT, adult Het used whisker to make significantly more contacts, spent more time investigating and had longer

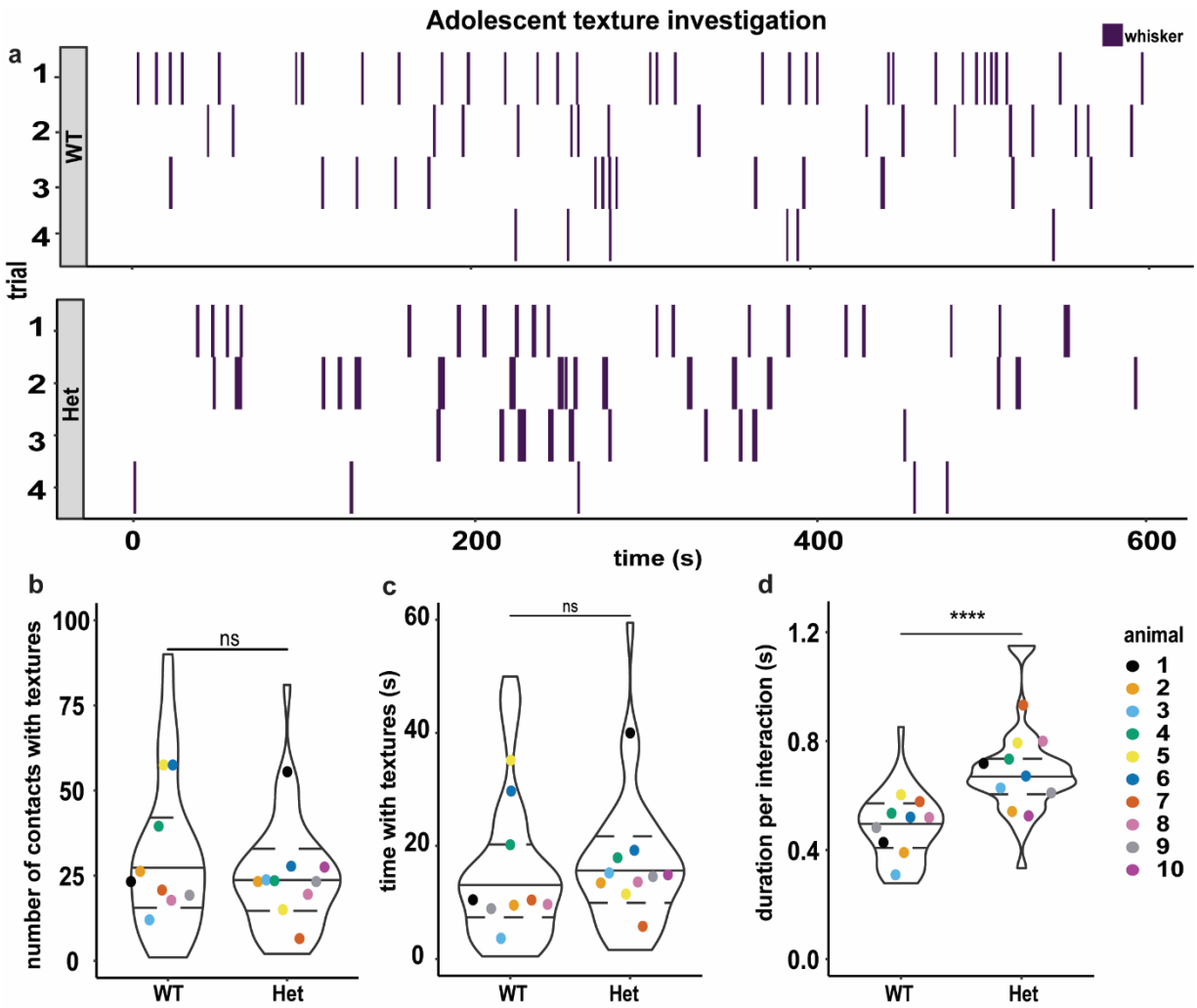

Figure 3. Adolescent Het have subtle whisking deficits during texture interactions. (**a.**) Examples of frame-by-frame texture interactions across four 10-min trials of texture exposure for adolescent WT (top panel) and Het (bottom panel), represented as sequences. The X- axis represents the time (s). Whisker interactions (purple) are plotted as blocks that span the duration of the interaction. Each row depicts fleeting whisker interactions of a mouse during individual trials. **(b-d.)** Statistical analysis of the interaction quantifications revealed that on average, WT and Het had similar total number of contacts across 4 trials (b.) and spent similar averaged total time investigating textures across 4 trials (c.). However, Het spent significantly longer during each whisker interaction than WT (d.). Superplots show animals color coded by circles, represent the mean of 4 trials (N=10 WT, N=9 Het). Superimposition of violin plots show median and distribution of all interactions. *Mann-Whitney test: ns = not significant, ****p < 0.0001.*

durations per whisker interaction with textures (Figure 5b, e, h). Adult Het also used forepaws and whole body climbing to significantly make more contacts, spent more time investigating and had longer time per interaction with textures than adult WT (Figure 5c-d, f-g, i-j). These findings are similar to previous studies in whiskerless and barrel-less mice (Guic-Robles et al., 1992; Guić-Robles et al., 1989) and suggest adult Het are seeking compensatory tactile sensation due to deficits in whisker sensation. Furthermore, this systematic analysis captures the individual variation expected in adult Het phenotypes, due to random X-chromosome inactivation patterns. Adult Het 3 and 5 (Figure 5b-d,h-j, light blue and yellow colors respectively), are similar to adult WT in number and duration of contacts with whiskers, and no interactions with forepaw or whole body, suggesting a likely normal S1BF, similar to

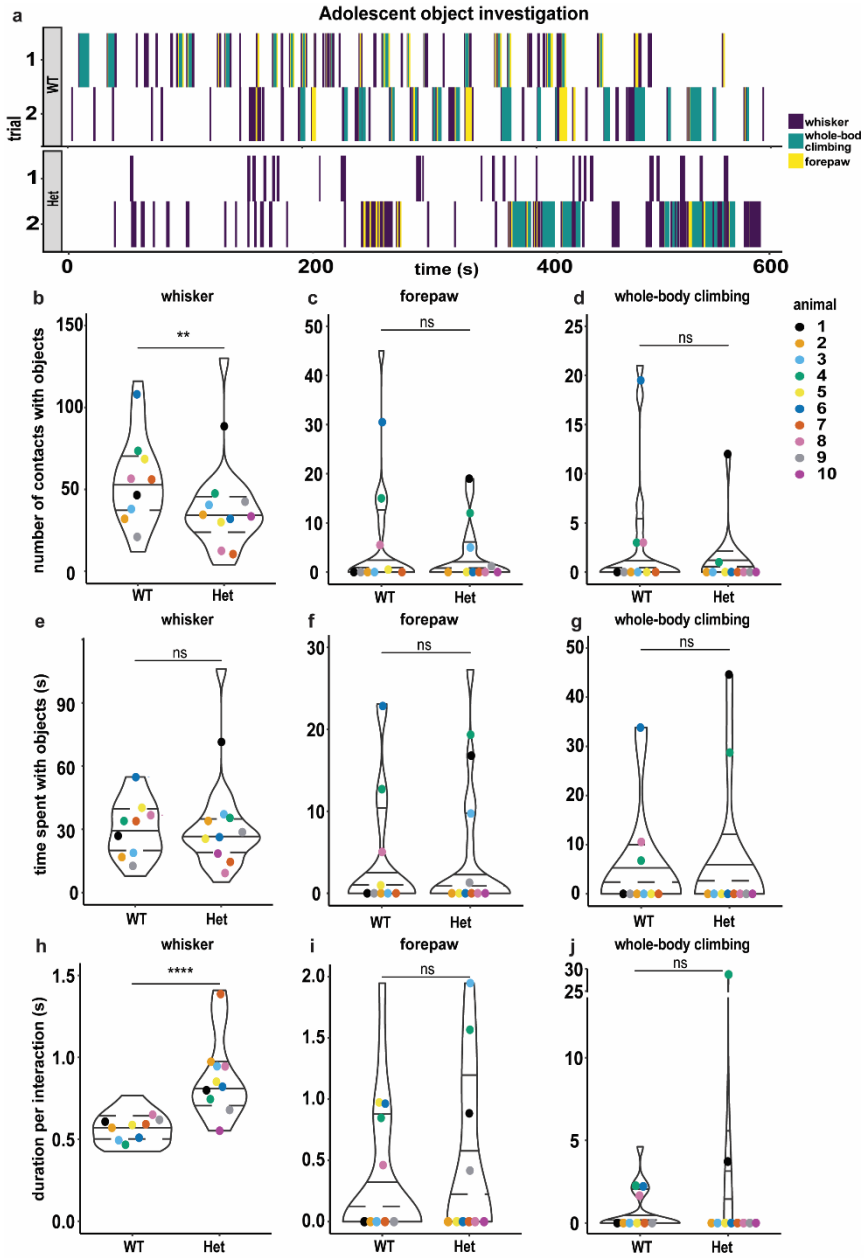

Figure 4. Adolescent Het exhibit subtle whisking deficits during object interactions (a.) Examples of frame-by-frame texture interactions across two 10-min trials of object exposure for adolescent WT (top panel) and Het (bottom panel) color coded by types of interaction (whisker, forepaw, whole-body climbing), represented as sequences. The X-axis represents the time (s) and interactions are plotted as blocks that span the duration of the interaction. Each row depicts fleeting whisker (purple), forepaw (yellow) or whole-body climbing (teal) interactions of the mice during individual trials. (**b-d.**) Statistical analysis of the interaction quantifications revealed Het made significantly more contacts using whisker (b.) but not forepaw (c.) or whole-body climbing (d.) compared to WT. **(e-g.)** There were no statistical differences between WT and Het for the time spent with objects using whisker (e), forepaw (f) or whole-body climbing (g). **(h-j.)** Het spent significantly more time than WT during each whisker interaction (h) but not with forepaw (i) or whole-body climbing (j). **(b-j.)** Superplots show animals color coded by circles, represent the mean of 2 trials (N=10 WT, N=9 Het). Superimposition of violin plots show mean and distribution of all itneractions. *Mann-Whitney test: ns = not significant, **p < 0.01, ****p < 0.0001.*

adult WT. Adult Het 6 and 7 (dark blue and deep orange respectively) perform forepaw interactions, but not whole body climbing (Figure 5c, d, f, g, i, j), suggesting minor sensory processing deficits in S1BF, which might be compensated by appropriate tactile perception of the forelimb region of the primary somatosensory cortex. The other five adult Het, which are most different from adult WT in their texture interactions, likely have profound deficits in neural processing in S1BF.

Surprisingly, adult Het had milder phenotypes while interacting with objects (Figure 6). Unlike texture investigations in adults, both adult WT and Het also used forepaws and whole-body climbing to interact with objects (Figure 6a). We did not observe significant differences in total number of contacts with objects and time spent investigating objects between adult WT and Het during whisker, forepaw or whole-body climbing interactions (Figure 6b-g). Adult Het spent significantly longer time per interaction with objects by using

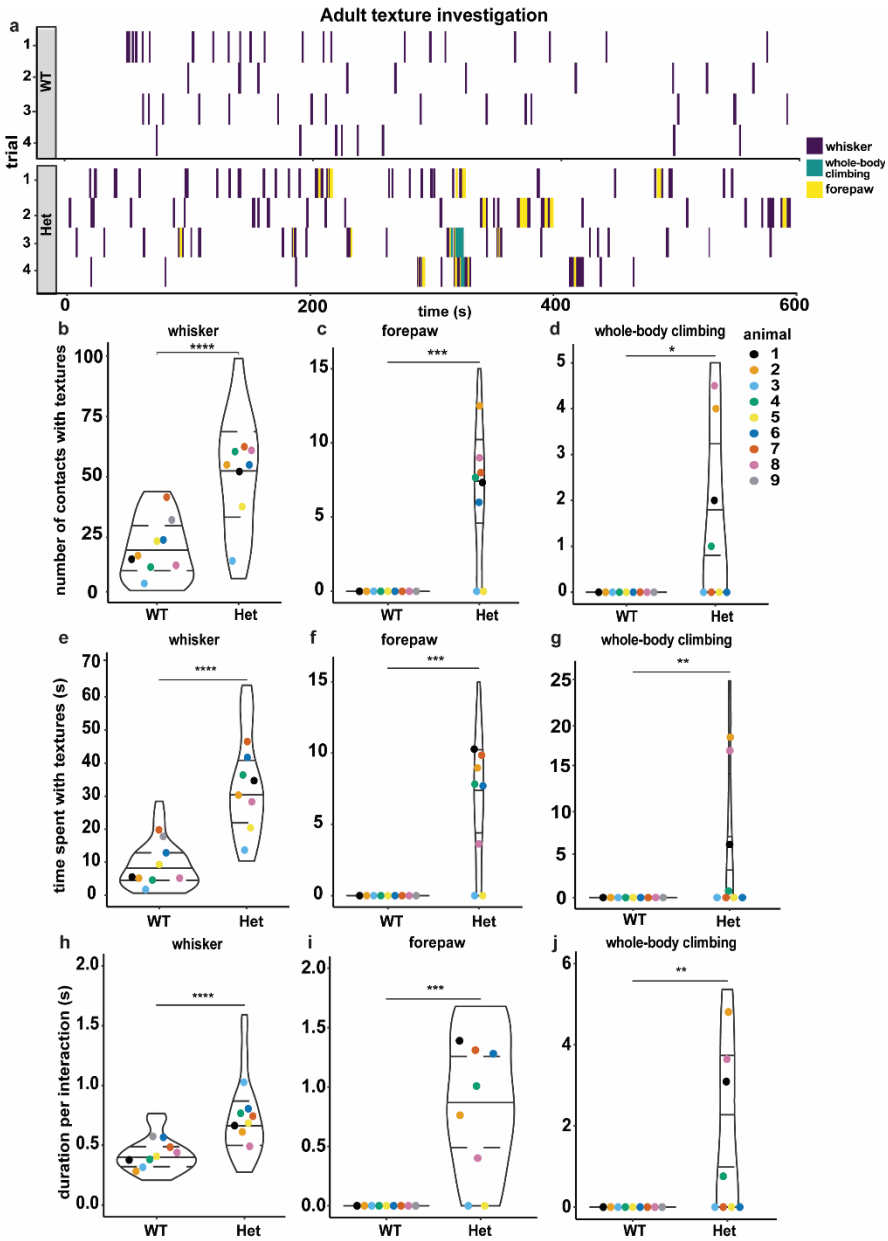

Figure 5. Adult Het exihibit hyposenstivity and compensatory behaviors during texture interactions. (a.) Examples of frame-by-frame texture interactions across four 10-min trials of object exposure for adult WT (top panel) and Het (bottom panel) color coded by types of interaction (whisker, forepaw, whole-body climbing), represented as sequences. The X-axis represents the time (s) and interactions are plotted as blocks that span the duration of the interaction. Each row depicts fleeting whisker (purple), forepaw (yellow) or whole-body climbing (teal) interactions of the mice during individual trials. **(b-j.)** Statistical analysis of the interaction quantifications revealed adult Het made significantly more contacts (b-d), spent significantly more total time (e-g) and time per interaction (h-j) with textures, with all interaction types (e-g), compared to adult WT. Superplots show animals color coded by circles, represent the mean of four trials (N=10 WT, N=9 Het). Superimposition of violin plots shows median and distibution of all interactions. *Mann-Whitney test: *p < 0.05, **p < 0.01, ***p < 0.001, ****p < 0.0001.*

whiskers (Figure 6h), but not forepaws and whole-body climbing (Figure 6i, j). Taken together, results from systematic analysis of texture investigation and object investigation across adolescent and adulthood point to the beginnings of regression in specific tactile sensory perception in 6-week-old female Het, with severe tactile hyposensitivity by 12 weeks of age.

Context-specific developmental progression in WT and regression in Het:

To develop a baseline in tactile performance in females over adolescence and adulthood, we compared within genotype across age. Compared to adolescent WT, we found that adult WT spent significantly lesser time with textures (Figure 7a, b), while the number of contacts remained similar (Figure 7c). On the other hand, compared to adolescent Het, adult Het spent significantly more time with textures and more numbers of contacts (Figure 7d,f), while the duration per contact remained similar (Figure 7e) Together, these results suggest a progression in whisker tactile interaction over age in WT, while Het

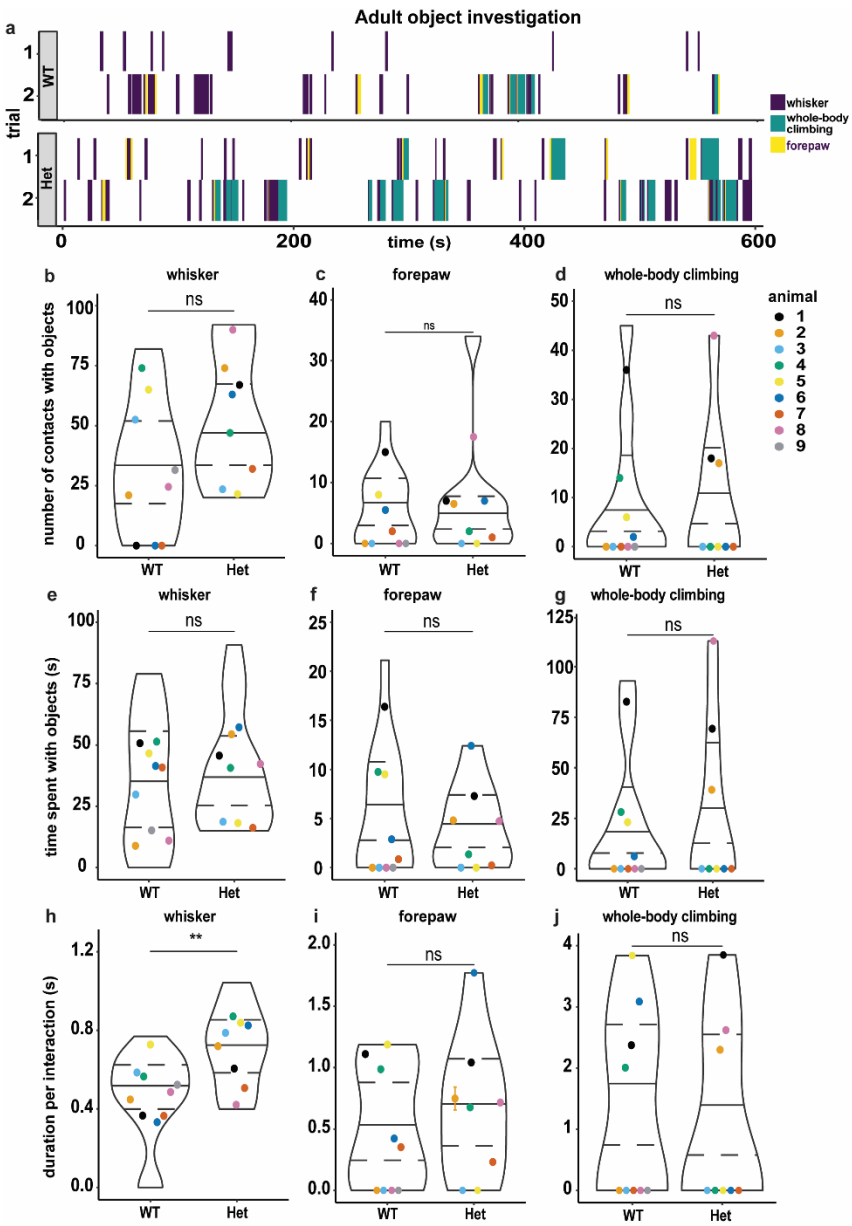

Figure 6. Adult Het display mild whisker deficit while interacting with objects. (a.) Examples of frame-by-frame texture interactions across two 10-min trials of object exposure for adult WT (top panel) and Het (bottom panel) color coded by types of interaction (whisker, forepaw, whole-body climbing), represented as sequences. The X-axis represents the time (s) and interactions are plotted as blocks that span the duration of the interaction. Each row depicts fleeting whisker (purple), forepaw (yellow) or whole-body climbing (teal) interactions of the mice during individual trials. (**b-j.**) Statistical analysis of the interaction quantifications revealed adult Het interacted with objects using whisker, forepaw and whole-body climbing, similar to WT, in the number of contacts (b-d), total time with objects (e-g) and time per interactions (h-j). Superplots show animals color coded by circles, represent the mean of 2 trials (n=10 WT, n=9 Het). Superimposition of violin plots show mean of distribution of all interactions. Statistical significance determined by non-parametric *Mann-Whitney test* $*p < 0.05$, $**p < 0.01$.

display a regression by the same parameters. Interestingly, neither WT nor Het showed any significant age-specific changes in interactions with objects (Figure 8a-f), suggesting that female mice may use different strategies while interacting with finer textures and objects.

No changes in perineuronal net expression in S1BF of adolescent Het

We previously reported that adult Het have atypical increased expression of mature high intensity perineuronal nets (PNNs), which are specialized extracellular matrix structures that restrict synaptic plasticity (Carstens et al., 2016; de Vivo et al., 2013; Pizzorusso et al., 2002), in the S1BF (Lau et al., 2020b). We proposed that the increased PNN expression could lead to poor performance in pup retrieval behavior by the adult Het (Lau et al., 2020b; Stevenson et al., 2021). Given the mild tactile phenotypes in adolescent Het, we sought to determine the status of PNN expression in adolescent Het S1BF. Using serial sectioning of entire S1BF and immunofluorescent staining of PNNs using Wisteria Floribunda agglutinin, we manually counted and analyzed high-intensity PNN expression (Figure 9 a, b). We

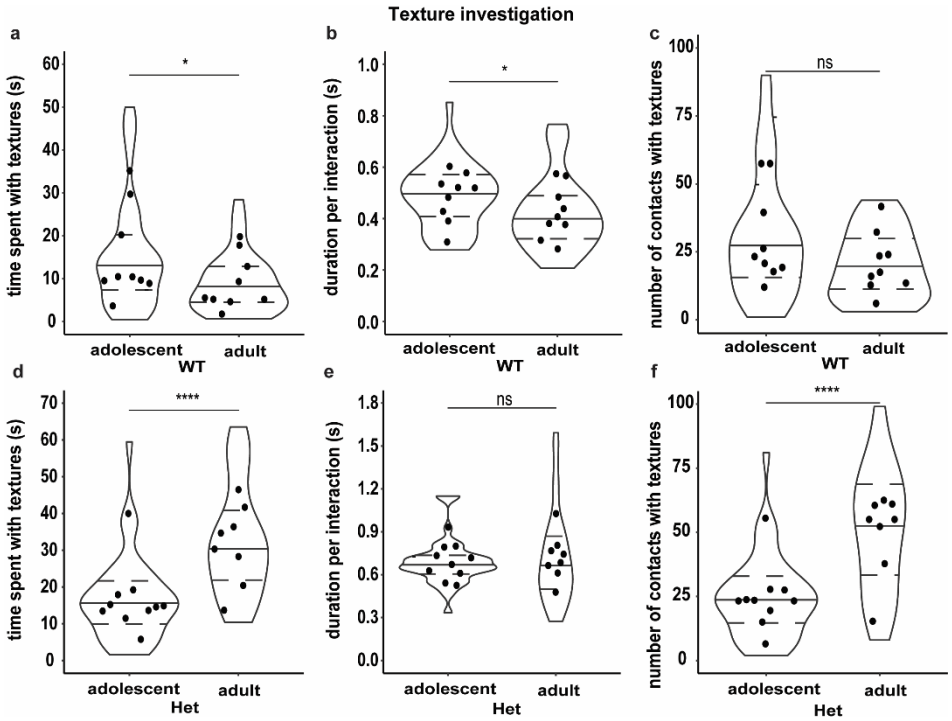

Figure 7. Differential age-specific changes in WT and Het texture interaction (a-c.) Using whiskers, adult WT interacted significantly longer (a: total time, b: time per interaction) with textures than adolescent WT, without changes in number of contacts made. **(d-f.)** However, adults Het used whiskers to significantly spent longer time (a: total time) and made more contacts (f) with textures than adolescent Het, without changes in time spent per interaction (e). Superplots represent the mean of 4 trials (adolescent: n=9 WT, n=10 Het; adult: n=9 WT, n=8 Het). Superimposition of violin plots show median and distribution of all interactions. *Mann-Whitney test: ns = not significant, *p < 0.05, ****p < 0.0001.*

found no significant differences in high-intensity PNN expression in S1BF between adolescent WT and Het across the rostro-caudal axis (Figure 9c, d). We also did not observe any significant differences in left-right asymmetry in PNN expression (WT-L: 12.845% +/- 1.607, n=6 :: WT-R: 18.315+/- 1.016 :: Het-L: 13.241+/- 0.380 :: Het-R: 14.932+/- .347) that we previously reported in adult WT and Het (Lau et al., 2020b). Together, these results suggest a concordance between high-intensity PNN expression and tactile sensory behaviors in Het over time.

Discussion:

Although diagnosed due to complex phenotypes such as regression in learned skills, there is increasing evidence that disrupted sensory processing is possibly a cause of many of the behavioral symptoms in neurodevelopmental disorders. Here, we use a well-established model of whisker tactile sensory perception to discover the impact of mosaic MECP2 expression in identified cell types and developmental stages in a female mouse model for Rett syndrome. These results set the stage to explore the mechanistic links between age dependent compensatory changes in MECP2 expression to neural circuitry involved in tactile sensory perception during simple and complex behavioral tasks in adolescent and adult Het.

One of the most intriguing results from this work is change in expression of MECP2 in Layer IV non-PV neurons in the S1BF of adolescent and adult Het. The observation that MECP2-expressing non-PV nuclei of S1BF have the ability to modulate MECP2 levels, and that MECP2 expression is not stable or static in adolescence or adulthood, provides new avenues for consideration in Het pathogenesis. To date, Rett syndrome is thought to be caused by ~50% of cells not expressing MECP2. However, our current results suggest that another cause could be

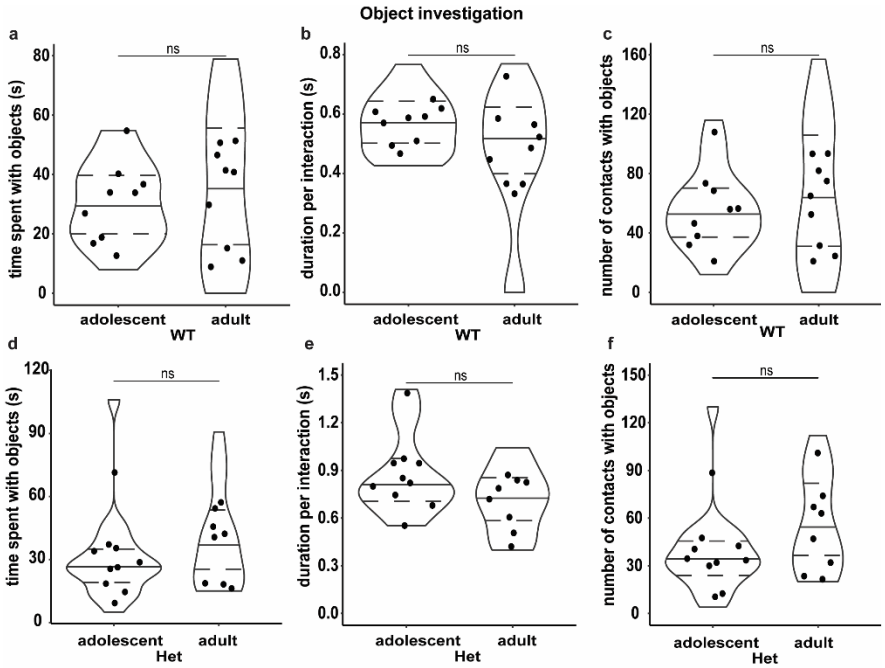

Figure 8. No differential age-specific changes in WT and Het object interaction (a-c.) Both adolescent and adults WT used whiskers similarly to interact with objects, as determined by total time spent (a), time per interaction (b) and number of contacts (c). **(d-f)** Comparably, adolescent and adult Het used whiskers similarly to interact with objects (d: total time; e: time per interaction; f: number of contacts). Superplots represent the mean of 2 trials (adolescent: n=9 WT, n=10 Het; adult: n=9 WT, n=8 Het). Superimposition of violin plots show median and distribution of interactions. *Mann-Whitney test: ns = not significant.*

the fluctuating levels of MECP2 from the ~50% of cells that are capable of expressing the wild-type protein. Thus, the early increase in MECP2 in non-PV cells in adolescence could be compensation for the lack of MECP2 protein in half of the cells; however, by adulthood, this increase is not maintained by the cells expressing MECP2. Thus, though the genotype and the cellular status of the Het remain the same through ages, their MECP2 expression levels are changing, suggesting in-built homeostatic mechanisms to regulate MECP2 expression in a cell type specific manner. This could be a basis for normal development in infancy and then regression in girls with Rett syndrome, as speculated by Dr. Jeff Neul (Neul, 2019). It is equally intriguing that PV neurons, with basal higher MECP2 expression, do not show these fluctuations across age in this naive state. The underlying mechanisms regulating MECP2 expression levels within cell types and ages is unclear and the subject of further investigation in our laboratory. We are also actively working on identifying the accurate cell type and lineage of these non-PV neurons.

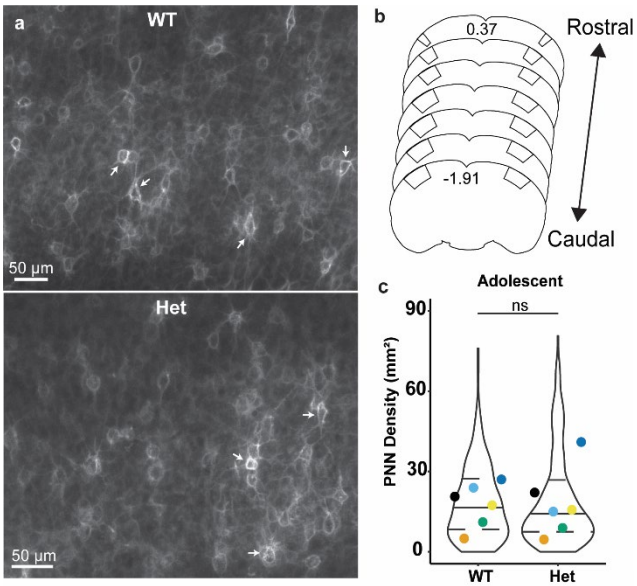

Figure 9. Adolescent Het show similar PNN density as WT within the barrel field of the primary somatosensory cortex. (a.) Schema of coronal mouse brain sections, depicting rostral (Bregma: 0.37 mm) to caudal (Bregma: -1.91 mm,) regions of S1BF analyzed for this study. Coordinate maps are based on Paxinos and Franklin's mouse brain atlas, 4th edition. **(b, c.)** Epifluorescent 10x micrographs of PNNs in S1BF of adolescent **(b)** WT and **(c)** Het. Arrows indicate high-intensity PNNs quantified for analysis. (**d.**) Statistical analysis of manually counted high-intense PNNs revealed that the density is similar between adolescent WT and Het within S1BF. Superplots show individual brains in different colors. Each circle represents the average high-intensity PNN density for that brain, superimposed on violin plots showing median with distirbution of all sections. WT: n=307 images, 6 animals. Het: n=313 images, 6 animals. *Mann-Whitney test: ns = not significant.*

MECP2 expression changes in appropriate primary sensory cortices in early developmental critical periods (He et al., 2014; Krishnan et al., 2015; Skene et al., 2010; Yagasaki et al., 2018). MECP2 expression in adolescence and adulthood are thought to be stable. However, systematic studies with cell-type specific fluorescent-assisted cell sorting over brain regions, ages, and experimental conditions are required to determine the extent of the dynamic range of MECP2 expression. Does the expression level of MECP2 matter for its nuclear functions of binding methylated DNA and regulating gene expression? Though not thoroughly investigated at the mechanistic level, increasing MECP2 expression in transgenic over-expression rodent lines or deleting MECP2 in specific cell types also largely results in Rett syndrome-like phenotypes at behavioral and cellular levels (Bhattacherjee et al., 2017; Chapleau et al., 2009; Goffin et al., 2014; He et al., 2014; Ito-Ishida et al., 2015; Meng et al., 2016; Mossner et al., 2020). Thus, it is plausible that regulation of MECP2 expression is critical for proper function and maintenance of the brain. However, considering the possibility of compensatory changes in MECP2 expression, it is critical to determine the impact of these manipulations on MECP2 expression in unmanipulated/non-target cells, in an age-specific manner.

Analysis of behavioral assays to study tactile sensory perception in female mice:

Traditionally, texture discrimination and object recognition assays are reported as percent novelty recognition, which is calculated as time spent investigating the novel texture/object divided by the total time spent investigating both textures/objects (Antunes & Biala, 2012; Ennaceur et al., 2005; Ennaceur & Delacour, 1988). This type of reporting normalizes the time spent investigating across individual animals to control for variation in exploration time. It is hypothesized that mice will spend more time with novel texture/object due to their innate nature of curiosity, and their ability to remember old or novel objects/textures from such interactions. However, a growing body of studies show that free-moving rodents do not have a preference for novelty (Antunes & Biala, 2012; Cohen & Stackman Jr., 2015; Ennaceur, 2010). Mice and rats show preference for familiar objects rather than novel objects (Ennaceur, 2010). Adult C57BL6 male mice show novelty object preference, whereas C57BL6 adult females show no preference between a familiar or novel object, consistent with our findings (Frick & Gresack, 2003). Thus, to reconcile these differences in the literature and establish first order metrics for analysis, we performed a systematic frame-by-frame analysis of interactions with textures and objects for adolescent and adult female mice of C57/Bl6 mice. By analyzing number and time of interactions, we found that adult WT require lesser time for interaction with textures, compared to adolescent WT females. On the other hand, adult Het interacted more and longer than adolescent Het, suggesting tactile hyposensitivity in adult Het. Together, these results suggest a regression in tactile interactions from 6-weeks to 12-weeks in Het. However, percentage of novelty recognition in textures or objects did not change in adolescent or adult WT or Het female mice. Thus, we refrain from speculating about preferences of the female mice or their memory.

Tactile hypersensitivity has been reported, based on change in novelty preferences in texture discrimination, novel object recognition and in social interactions in male null mice, and mice with conditional deletion of *Mecp2* in peripheral somatosensory neurons (Ito-Ishida et al., 2015; Orefice et al., 2016). Removal of MECP2 from forebrain pyramidal neurons results in tactile hyposensitivity (Chao et al., 2010; Ito-Ishida et al., 2015). The differences in age, sex, strain, and experimental methods and data analysis between these studies and our own make it difficult to reconcile these findings. Yet, it is clear that MECP2 expression is essential for proper functioning of neuronal circuits involved in tactile sensory perception.

Perineuronal nets and PV-pyramidal networks in Mecp2-deficient mouse models:

We have previously shown that adult Het mice have increased and atypical expression of PNNs perineuronal nets in auditory cortex (Krishnan et al., 2017) and specific sub-regions of the primary somatosensory cortex (Lau et al., 2020b). Typically, pup vocalizations trigger suppression of parvalbumin+ GABAergic neuronal responses and a concomitant disinhibition in deep-layer pyramidal neurons in the auditory cortex of adult WT surrogates (Lau et al., 2020a). In adult Het surrogates, the increased perineuronal net expression interferes with the synaptic plasticity of parvalbumin+ GABAergic neurons, which ultimately result in lack of disinhibition of the pyramidal neurons (Lau et al., 2020a). It is currently unknown if similar mechanisms also occur in the primary somatosensory cortex, and in an age-dependent manner, which would ultimately lead to atypical tactile processing in adult Het and not in the adolescent Het.

Rehabilitation strategies:

Recent work indicates that early interventions aimed at increasing neuronal activity mitigate disease onset in male and female mouse models for Rett syndrome. Early administration of Ampakine CX546, a positive modulator of AMPA receptors, from P3-P9 in Mecp2 null mice enhances neuronal activity, prolongs lifespan, delays disease progression, and rescues motor abilities and spatial memory (Scaramuzza et al., 2021). In Het females, repetitive training enhances neuronal activity of task-specific neurons and improves both spatial memory and motor function well into adulthood (Achilly et al., 2021). Adolescent and adult Het improves their pup retrieval behavior with repeated trials over days, compared to non-consecutive days of training (Krishnan et al., 2017; Stevenson et al., 2021). Early and repetitive training overall delays the onset of disease phenotypes and improves the latency to survival in Het, reiterating the plasticity capacity of the Het brain. We speculate that MECP2 expression is affected by these trainings, especially at earlier age, resulting in activation of compensation pathways leading to behaviors that are more typical. Different mechanisms are likely at play in maintaining this compensation. Further work is needed to identify therapeutic and rehabilitative strategies targeting maintenance of this compensation in female Het brains for mitigating disease progression throughout life.

Acknowledgements:

We would like to thank undergraduates Beyza Kartal, Benjamin Bridges, Trinity Rose Shultz and Sami Issac for help in performing maternal behavior. We would also like to thank undergraduates Beyza Kartal, Shahin Ahmadi, Itzanami Sotelo Hernandez, Deema Mansour, Abrielle Noyes and Ansley Houston from the UTK SURGE program, and the 2020 and 2021 BCMB 420 Image analysis class for help in mapping and analyzing high intensity PNN data. We would like to thank the lab of Dr. Maitreyi Das and her graduate students for training and assistance using their confocal microscope. This work was supported by BCMB Chancellors fellowship (MM and DLC), 2021 Office of Research, Innovation, and Economic Development (ORIED) Scholarly and Research Incentive Funds (SARIF) (MM), BCMB James and Dora Wright Fellowship (MM), postdoctoral fellowship award from Rettsyndrome.org (BYBL), startup funds from the University of Tennessee—Knoxville (KK), and by the National Institutes of Mental Health of the National Institutes of Health under Award Number R15MH124042 (KK).

References:

Achilly, N. P., Wang, W., & Zoghbi, H. Y. (2021). Presymptomatic training mitigates functional deficits in a mouse model of Rett syndrome. *Nature*, *592*(7855), 596–600. https://doi.org/10.1038/s41586-021-03369-7

Amir, R. E., Van den Veyver, I. B., Wan, M., Tran, C. Q., Francke, U., & Zoghbi, H. Y. (1999). Rett syndrome is caused by mutations in X-linked MECP2, encoding methyl-CpG-binding protein 2. *Nature Genetics*, *23*(2), 185–188. https://doi.org/10.1038/13810

Antunes, M., & Biala, G. (2012). The novel object recognition memory: Neurobiology, test procedure, and its modifications. *Cognitive Processing*, *13*(2), 93–110. https://doi.org/10.1007/s10339-011-0430-z

Bebbington, A., Anderson, A., Ravine, D., Fyfe, S., Pineda, M., de Klerk, N., Ben-Zeev, B., Yatawara, N., Percy, A., Kaufmann, W. E., & Leonard, H. (2008). Investigating genotype-phenotype relationships in Rett syndrome using an international data set. *Neurology*, *70*(11), 868–875. https://doi.org/10.1212/01.wnl.0000304752.50773.ec

Bhattacherjee, A., Mu, Y., Winter, M. K., Knapp, J. R., Eggimann, L. S., Gunewardena, S. S., Kobayashi, K., Kato, S., Krizsan-Agbas, D., & Smith, P. G. (2017). Neuronal cytoskeletal gene dysregulation and mechanical hypersensitivity in a rat model of Rett syndrome. *Proceedings of the National Academy of Sciences*, *114*(33). https://doi.org/10.1073/pnas.1618210114

Braunschweig, D. (2004). X-Chromosome inactivation ratios affect wild-type MeCP2 expression within mosaic Rett syndrome and Mecp2-/+ mouse brain. *Human Molecular Genetics*, *13*(12), 1275–1286. https://doi.org/10.1093/hmg/ddh142

Buchanan, C. B., Stallworth, J. L., Scott, A. E., Glaze, D. G., Lane, J. B., Skinner, S. A., Tierney, A. E., Percy, A. K., Neul, J. L., & Kaufmann, W. E. (2019). Behavioral profiles in Rett syndrome: Data from the natural history study. *Brain and Development*, *41*(2), 123–134. https://doi.org/10.1016/j.braindev.2018.08.008

Carstens, K. E., Phillips, M. L., Pozzo-Miller, L., Weinberg, R. J., & Dudek, S. M. (2016). Perineuronal Nets Suppress Plasticity of Excitatory Synapses on CA2 Pyramidal Neurons. *The Journal of Neuroscience*, *36*(23), 6312–6320. https://doi.org/10.1523/JNEUROSCI.0245-16.2016

Chahrour, M., Jung, S. Y., Shaw, C., Zhou, X., Wong, S. T. C., Qin, J., & Zoghbi, H. Y. (2008). MeCP2, a Key Contributor to Neurological Disease, Activates and Represses Transcription. *Science*, *320*(5880), 1224–1229. https://doi.org/10.1126/science.1153252

Chao, H.-T., Chen, H., Samaco, R. C., Xue, M., Chahrour, M., Yoo, J., Neul, J. L., Gong, S., Lu, H.-C., Heintz, N., Ekker, M., Rubenstein, J. L. R., Noebels, J. L., Rosenmund, C., & Zoghbi, H. Y. (2010). Dysfunction in GABA signalling mediates autism-like stereotypies and Rett syndrome phenotypes. *Nature*, *468*(7321), 263–269. https://doi.org/10.1038/nature09582

Chapleau, C. A., Calfa, G. D., Lane, M. C., Albertson, A. J., Larimore, J. L., Kudo, S., Armstrong, D. L., Percy, A. K., & Pozzo-Miller, L. (2009). Dendritic spine pathologies in hippocampal pyramidal neurons from Rett syndrome brain and after expression of Rett-associated MECP2 mutations. *Neurobiology of Disease*, *35*(2), 219–233. https://doi.org/10.1016/j.nbd.2009.05.001

Chen, L., Chen, K., Lavery, L. A., Baker, S. A., Shaw, C. A., Li, W., & Zoghbi, H. Y. (2015). MeCP2 binds to non-CG methylated DNA as neurons mature, influencing transcription and the timing of onset for Rett syndrome. *Proceedings of the National Academy of Sciences*, *112*(17), 5509–5514. https://doi.org/10.1073/pnas.1505909112

Cohen, S. J., & Stackman Jr., R. W. (2015). Assessing rodent hippocampal involvement in the novel object recognition task. A review. *Behavioural Brain Research*, *285*, 105–117. https://doi.org/10.1016/j.bbr.2014.08.002

Datavyu Team. (2014). *Datavyu: A video coding tool. Databrary project*. Datavyu Team.

de Vivo, L., Landi, S., Panniello, M., Baroncelli, L., Chierzi, S., Mariotti, L., Spolidoro, M., Pizzorusso, T., Maffei, L., & Ratto, G. M. (2013). Extracellular matrix inhibits structural and functional plasticity of dendritic spines in the adult visual cortex. *Nature Communications*, *4*(1), 1484. https://doi.org/10.1038/ncomms2491

Djukic, A., & Valicenti McDermott, M. (2012). Social Preferences in Rett Syndrome. *Pediatric Neurology*, *46*(4), 240–242. https://doi.org/10.1016/j.pediatrneurol.2012.01.011

Djukic, A., Valicenti McDermott, M., Mavrommatis, K., & Martins, C. L. (2012). Rett Syndrome: Basic Features of Visual Processing—A Pilot Study of Eye-Tracking. *Pediatric Neurology*, *47*(1), 25–29. https://doi.org/10.1016/j.pediatrneurol.2012.04.009

Durand, S., Patrizi, A., Quast, K. B., Hachigian, L., Pavlyuk, R., Saxena, A., Carninci, P., Hensch, T. K., & Fagiolini, M. (2012). NMDA Receptor Regulation Prevents Regression of Visual Cortical Function in the Absence of Mecp2. *Neuron*, *76*(6), 1078–1090. https://doi.org/10.1016/j.neuron.2012.12.004

Ennaceur, A. (2010). One-trial object recognition in rats and mice: Methodological and theoretical issues. *Behavioural Brain Research*, *215*(2), 244–254. https://doi.org/10.1016/j.bbr.2009.12.036

Ennaceur, A., & Delacour, J. (1988). A new one-trial test for neurobiological studies of memory in rats. 1: Behavioral data. *Behavioural Brain Research*, *31*(1), 47–59. https://doi.org/10.1016/0166-4328(88)90157-X

Ennaceur, A., Michalikova, S., Bradford, A., & Ahmed, S. (2005). Detailed analysis of the behavior of Lister and Wistar rats in anxiety, object recognition and object location tasks. *Behavioural Brain Research*, *159*(2), 247–266. https://doi.org/10.1016/j.bbr.2004.11.006

Frick, K. M., & Gresack, J. E. (2003). Sex Differences in the Behavioral Response to Spatial and Object Novelty in Adult C57BL/6 Mice. *Behavioral Neuroscience*, *117*(6), 1283–1291. https://doi.org/10.1037/0735-7044.117.6.1283

Fuks, F., Hurd, P. J., Wolf, D., Nan, X., Bird, A. P., & Kouzarides, T. (2003). The Methyl-CpG-binding Protein MeCP2 Links DNA Methylation to Histone Methylation. *Journal of Biological Chemistry*, *278*(6), 4035–4040. https://doi.org/10.1074/jbc.M210256200

Gabel, H. W., Kinde, B., Stroud, H., Gilbert, C. S., Harmin, D. A., Kastan, N. R., Hemberg, M., Ebert, D. H., & Greenberg, M. E. (2015). Disruption of DNA-methylation-dependent long gene repression in Rett syndrome. *Nature*, *522*(7554), 89–93. https://doi.org/10.1038/nature14319

Goffin, D., Brodkin, E. S., Blendy, J. A., Siegel, S. J., & Zhou, Z. (2014). Cellular origins of auditory event-related potential deficits in Rett syndrome. *Nature Neuroscience*, *17*(6), 804–806. https://doi.org/10.1038/nn.3710

Guic-Robles, E., Jenkins, W. M., & Bravo, H. (1992). Vibrissal roughness discrimination is barrelcortex-dependent. *Behavioural Brain Research*, *48*(2), 145–152. https://doi.org/10.1016/S0166-4328(05)80150-0

Guić-Robles, E., Valdivieso, C., & Guajardo, G. (1989). Rats can learn a roughness discrimination using only their vibrissal system. *Behavioural Brain Research*, *31*(3), 285–289. https://doi.org/10.1016/0166-4328(89)90011-9

Guy, J., Hendrich, B., Holmes, M., Martin, J. E., & Bird, A. (2001). A mouse Mecp2-null mutation causes neurological symptoms that mimic Rett syndrome. *Nature Genetics*, *27*(3), 322–326. https://doi.org/10.1038/85899

Hartig, W., Brauer, K., & Bruckner, G. (1992). Wisteria floribunda agglutinin-labelled nets surround parvalbumin-containing neurons. *Neuroreport*, *3*(10), 869–872.

He, L., Liu, N., Cheng, T., Chen, X., Li, Y., Shu, Y., Qiu, Z., & Zhang, X. (2014). Conditional deletion of Mecp2 in parvalbumin-expressing GABAergic cells results in the absence of

critical period plasticity. *Nature Communications*, *5*(1), 5036. https://doi.org/10.1038/ncomms6036

Ito-Ishida, A., Ure, K., Chen, H., Swann, J. W., & Zoghbi, H. Y. (2015). Loss of MeCP2 in Parvalbumin-and Somatostatin-Expressing Neurons in Mice Leads to Distinct Rett Syndrome-like Phenotypes. *Neuron*, *88*(4), 651–658. https://doi.org/10.1016/j.neuron.2015.10.029

Jones, P. L., Veenstra, G. J. C., Wade, P. A., Vermaak, D., Kass, S. U., Landsberger, N., Strouboulis, J., & Wolffe, A. P. (1998). Methylated DNA and MeCP2 recruit histone deacetylase to repress transcription. *Nature Genetics*, *19*(2), 187–191. https://doi.org/10.1038/561

Key, A. P., Jones, D., & Peters, S. (2019). Spoken word processing in Rett syndrome: Evidence from event-related potentials. *International Journal of Developmental Neuroscience*, *73*(1), 26–31. https://doi.org/10.1016/j.ijdevneu.2019.01.001

Klose, R. J., Sarraf, S. A., Schmiedeberg, L., McDermott, S. M., Stancheva, I., & Bird, A. P. (2005). DNA Binding Selectivity of MeCP2 Due to a Requirement for A/T Sequences Adjacent to Methyl-CpG. *Molecular Cell*, *19*(5), 667–678. https://doi.org/10.1016/j.molcel.2005.07.021

Krishnan, K., Lau, B. Y. B., Ewall, G., Huang, Z. J., & Shea, S. D. (2017). MECP2 regulates cortical plasticity underlying a learned behaviour in adult female mice. *Nature Communications*, *8*(1), 14077. https://doi.org/10.1038/ncomms14077

Krishnan, K., Wang, B.-S., Lu, J., Wang, L., Maffei, A., Cang, J., & Huang, Z. J. (2015). MeCP2 regulates the timing of critical period plasticity that shapes functional connectivity in primary visual cortex. *Proceedings of the National Academy of Sciences*, *112*(34). https://doi.org/10.1073/pnas.1506499112

Lau, B. Y. B., Krishnan, K., Huang, Z. J., & Shea, S. D. (2020). Maternal Experience-Dependent Cortical Plasticity in Mice Is Circuit- and Stimulus-Specific and Requires MECP2. *The Journal of Neuroscience*, *40*(7), 1514–1526. https://doi.org/10.1523/JNEUROSCI.1964-19.2019

Lau, B. Y. B., Layo, D. E., Emery, B., Everett, M., Kumar, A., Stevenson, P., Reynolds, K. G., Cherosky, A., Bowyer, S.-A. H., Roth, S., Fisher, D. G., McCord, R. P., & Krishnan, K. (2020). Lateralized Expression of Cortical Perineuronal Nets during Maternal Experience is Dependent on MECP2. *Eneuro*, *7*(3), ENEURO.0500-19.2020. https://doi.org/10.1523/ENEURO.0500-19.2020

LeBlanc, J. J., DeGregorio, G., Centofante, E., Vogel-Farley, V. K., Barnes, K., Kaufmann, W. E., Fagiolini, M., & Nelson, C. A. (2015). Visual evoked potentials detect cortical processing deficits in Rett syndrome: VEP in Rett Syndrome. *Annals of Neurology*, *78*(5), 775–786. https://doi.org/10.1002/ana.24513

Lee, L.-J., Tsytsarev, V., & Erzurumlu, R. S. (2017). Structural and functional differences in the barrel cortex of *Mecp2* null mice. *Journal of Comparative Neurology*, *525*(18), 3951–3961. https://doi.org/10.1002/cne.24315

Lo, F.-S., Blue, M. E., & Erzurumlu, R. S. (2016). Enhancement of postsynaptic $GABA_A$ and extrasynaptic NMDA receptor-mediated responses in the barrel cortex of *Mecp2* -null mice. *Journal of Neurophysiology*, *115*(3), 1298–1306. https://doi.org/10.1152/jn.00944.2015

Lyst, M. J., & Bird, A. (2015). Rett syndrome: A complex disorder with simple roots. *Nature Reviews Genetics*, *16*(5), 261–275. https://doi.org/10.1038/nrg3897

Meng, X., Wang, W., Lu, H., He, L., Chen, W., Chao, E. S., Fiorotto, M. L., Tang, B., Herrera, J. A., Seymour, M. L., Neul, J. L., Pereira, F. A., Tang, J., Xue, M., & Zoghbi, H. Y. (2016). Manipulations of MeCP2 in glutamatergic neurons highlight their contributions to Rett and other neurological disorders. *ELife*, *5*, e14199. https://doi.org/10.7554/eLife.14199

Merbler, A. M., Byiers, B. J., Hoch, J., Dimian, A. C., Barney, C. C., Feyma, T. J., Beisang, A. A., Bartolomucci, A., & Symons, F. J. (2020). Preliminary Evidence That Resting State Heart Rate Variability Predicts Reactivity to Tactile Stimuli in Rett Syndrome. *Journal of Child Neurology*, *35*(1), 42–48. https://doi.org/10.1177/0883073819875915

Morello, N., Schina, R., Pilotto, F., Phillips, M., Melani, R., Plicato, O., Pizzorusso, T., Pozzo-Miller, L., & Giustetto, M. (2018). Loss of Mecp2 Causes Atypical Synaptic and Molecular Plasticity of Parvalbumin-Expressing Interneurons Reflecting Rett Syndrome–Like Sensorimotor Defects. *Eneuro*, *5*(5), ENEURO.0086-18.2018. https://doi.org/10.1523/ENEURO.0086-18.2018

Mossner, J. M., Batista-Brito, R., Pant, R., & Cardin, J. A. (2020). Developmental loss of MeCP2 from VIP interneurons impairs cortical function and behavior. *ELife*, *9*, e55639. https://doi.org/10.7554/eLife.55639

Neul, J. L. (2019). Can Rett syndrome be diagnosed before regression? *Neuroscience & Biobehavioral Reviews*, *104*, 158–159. https://doi.org/10.1016/j.neubiorev.2019.07.005

Nomura, Y. (2005). Early behavior characteristics and sleep disturbance in Rett syndrome. *Brain and Development*, *27*, S35–S42. https://doi.org/10.1016/j.braindev.2005.03.017

Noutel, J., Hong, Y. K., Leu, B., Kang, E., & Chen, C. (2011). Experience-Dependent Retinogeniculate Synapse Remodeling Is Abnormal in MeCP2-Deficient Mice. *Neuron*, *70*(1), 35–42. https://doi.org/10.1016/j.neuron.2011.03.001

Orefice, L. L., Zimmerman, A. L., Chirila, A. M., Sleboda, S. J., Head, J. P., & Ginty, D. D. (2016). Peripheral Mechanosensory Neuron Dysfunction Underlies Tactile and Behavioral Deficits in Mouse Models of ASDs. *Cell*, *166*(2), 299–313. https://doi.org/10.1016/j.cell.2016.05.033

Pacchiarini, N., Fox, K., & Honey, R. C. (2017). Perceptual learning with tactile stimuli in rodents: Shaping the somatosensory system. *Learning & Behavior*, *45*(2), 107–114. https://doi.org/10.3758/s13420-017-0269-y

Patrick Wu, H.-P., & Dyck, R. H. (2018). Signaling by Synaptic Zinc is Required for Whisker-Mediated, Fine Texture Discrimination. *Neuroscience*, *369*, 242–247. https://doi.org/10.1016/j.neuroscience.2017.11.020

Patrizi, A., Awad, P. N., Chattopadhyaya, B., Li, C., Di Cristo, G., & Fagiolini, M. (2020). Accelerated Hyper-Maturation of Parvalbumin Circuits in the Absence of MeCP2. *Cerebral Cortex*, *30*(1), 256–268. https://doi.org/10.1093/cercor/bhz085

Paxinos, G., & Franklin, K. B. J. (2013). *Paxino's and Franklin's The Mouse Brain In Stereotaxic Coordinates, 4th Ed* (Fourth). Academic Press.

Peters, S. U., Gordon, R. L., & Key, A. P. (2015). Induced Gamma Oscillations Differentiate Familiar and Novel Voices in Children With *MECP2* Duplication and Rett Syndromes. *Journal of Child Neurology*, *30*(2), 145–152. https://doi.org/10.1177/0883073814530503

Picard, N., & Fagiolini, M. (2019). MeCP2: An epigenetic regulator of critical periods. *Current Opinion in Neurobiology*, *59*, 95–101. https://doi.org/10.1016/j.conb.2019.04.004

Pizzorusso, T., Medini, P., Berardi, N., Chierzi, S., Fawcett, J. W., & Maffei, L. (2002). Reactivation of Ocular Dominance Plasticity in the Adult Visual Cortex. *Science*, *298*(5596), 1248–1251. https://doi.org/10.1126/science.1072699

Rodgers, C. C., Nogueira, R., Pil, B. C., Greeman, E. A., Park, J. M., Hong, Y. K., Fusi, S., & Bruno, R. M. (2021). Sensorimotor strategies and neuronal representations for shape discrimination. *Neuron*, *109*(14), 2308-2325.e10. https://doi.org/10.1016/j.neuron.2021.05.019

Scaramuzza, L., De Rocco, G., Desiato, G., Cobolli Gigli, C., Chiacchiaretta, M., Mirabella, F., Pozzi, D., De Simone, M., Conforti, P., Pagani, M., Benfenati, F., Cesca, F., Bedogni, F., & Landsberger, N. (2021). The enhancement of activity rescues the establishment of *Mecp2*

null neuronal phenotypes. *EMBO Molecular Medicine*, *13*(4). https://doi.org/10.15252/emmm.202012433

Schneider, C. A., Rasband, W. S., & Eliceiri, K. W. (2012). NIH Image to ImageJ: 25 years of image analysis. *Nature Methods*, *9*(7), 671–675. https://doi.org/10.1038/nmeth.2089

Skene, P. J., Illingworth, R. S., Webb, S., Kerr, A. R. W., James, K. D., Turner, D. J., Andrews, R., & Bird, A. P. (2010). Neuronal MeCP2 Is Expressed at Near Histone-Octamer Levels and Globally Alters the Chromatin State. *Molecular Cell*, *37*(4), 457–468. https://doi.org/10.1016/j.molcel.2010.01.030

Stevenson, P. K., Casenhiser, D. M., Lau, B. Y. B., & Krishnan, K. (2021). Systematic analysis of goal-related movement sequences during maternal behaviour in a female mouse model for Rett syndrome. *European Journal of Neuroscience*, *54*(2), 4528–4549. https://doi.org/10.1111/ejn.15327

Symons, F. J., Barney, C. C., Byiers, B. J., McAdams, B. D., Foster, S. X. Y. L., Feyma, T. J., Wendelschafer-Crabb, G., & Kennedy, W. R. (2019). A clinical case–control comparison of epidermal innervation density in Rett syndrome. *Brain and Behavior*, *9*(5), e01285. https://doi.org/10.1002/brb3.1285

Takei, Y., Zheng, S., Yun, J., Shah, S., Pierson, N., White, J., Schindler, S., Tischbirek, C. H., Yuan, G.-C., & Cai, L. (2021). Single-cell nuclear architecture across cell types in the mouse brain. *Science*, eabj1966. https://doi.org/10.1126/science.abj1966

Tao, J., Hu, K., Chang, Q., Wu, H., Sherman, N. E., Martinowich, K., Klose, R. J., Schanen, C., Jaenisch, R., Wang, W., & Sun, Y. E. (2009). Phosphorylation of MeCP2 at Serine 80 regulates its chromatin association and neurological function. *Proceedings of the National Academy of Sciences*, *106*(12), 4882–4887. https://doi.org/10.1073/pnas.0811648106

Ueno, H., Takao, K., Suemitsu, S., Murakami, S., Kitamura, N., Wani, K., Okamoto, M., Aoki, S., & Ishihara, T. (2018). Age-dependent and region-specific alteration of parvalbumin neurons and perineuronal nets in the mouse cerebral cortex. *Neurochemistry International*, *112*, 59–70. https://doi.org/10.1016/j.neuint.2017.11.001

Wu, H.-P. P., Ioffe, J. C., Iverson, M. M., Boon, J. M., & Dyck, R. H. (2013). Novel, whisker-dependent texture discrimination task for mice. *Behavioural Brain Research*, *237*, 238–242. https://doi.org/10.1016/j.bbr.2012.09.044

Yagasaki, Y., Miyoshi, G., & Miyata, M. (2018). Experience-dependent MeCP2 expression in the excitatory cells of mouse visual thalamus. *PLOS ONE*, *13*(5), e0198268. https://doi.org/10.1371/journal.pone.0198268

Zhou, Z., Hong, E. J., Cohen, S., Zhao, W., Ho, H. H., Schmidt, L., Chen, W. G., Lin, Y., Savner, E., Griffith, E. C., Hu, L., Steen, J. A. J., Weitz, C. J., & Greenberg, M. E. (2006). Brain-Specific Phosphorylation of MeCP2 Regulates Activity-Dependent Bdnf Transcription, Dendritic Growth, and Spine Maturation. *Neuron*, *52*(2), 255–269. https://doi.org/10.1016/j.neuron.2006.09.037